HHS Public Access

Author manuscript

Bone. Author manuscript; available in PMC 2020 January 01.

Published in final edited form as:

Bone. 2019 January ; 118: 32–41. doi:10.1016/j.bone.2018.01.016.

Bone marrow adipocytes resist lipolysis and remodeling in response to β-adrenergic stimulation

Erica L. Scheller[1,*], **Shaima Khandaker**[2], **Brian S. Learman**[2], **William P. Cawthorn**[3], **Lindsay M. Anderson**[2], **H. A. Pham**[2], **Hero Robles**[1], **Zhaohua Wang**[1], **Ziru Li**[2], **Sebastian D. Parlee**[2], **Becky R. Simon**[2], **Hiroyuki Mori**[2], **Adam J. Bree**[2], **Clarissa S. Craft**[1], and **Ormond A. MacDougald**[2,4,*]

[1]Division of Bone and Mineral Diseases, Department of Internal Medicine, Washington University, Saint Louis, Missouri 63110, USA

[2]Department of Molecular & Integrative Physiology, University of Michigan, Ann Arbor, Michigan 48105, USA

[3]BHF/University Centre for Cardiovascular Science, The Queen's Medical Research Institute, University of Edinburgh, Edinburgh, UK

[4]Department of Internal Medicine, University of Michigan, Ann Arbor, Michigan 48109, USA

Abstract

Bone marrow adipose tissue (BMAT) is preserved or increased in states of caloric restriction. Similarly, we found that BMAT in the tail vertebrae, but not the red marrow in the tibia, resists loss of neutral lipid with acute, 48-hour fasting in rats. The mechanisms underlying this phenomenon and its seemingly distinct regulation from peripheral white adipose tissue (WAT) remain unknown. To test the role of β-adrenergic stimulation, a major regulator of adipose tissue lipolysis, we examined the responses of BMAT to β-adrenergic agonists. Relative to inguinal WAT, BMAT had reduced phosphorylation of hormone sensitive lipase (HSL) after treatment with pan-β-adrenergic agonist isoproterenol. Phosphorylation of HSL in response to β3-adrenergic agonist CL316,243 was decreased by an additional ~90% (distal tibia BMAT) or could not be detected (tail vertebrae). *Ex vivo*, adrenergic stimulation of lipolysis in purified BMAT adipocytes was also substantially less than iWAT adipocytes and had site-specific properties. Specifically, regulated bone marrow adipocytes (rBMAs) from proximal tibia and femur underwent lipolysis in response to both CL316,243 and forskolin, while constitutive BMAs from the tail responded only to forskolin. This occurred independently of changes in gene expression of β-adrenergic receptors, which were similar between adipocytes from iWAT and BMAT, and could not be explained by defective coupling of β-adrenergic receptors to lipolytic machinery through caveolin 1.

[*]Corresponding Authors: Dr. Erica L Scheller, Department of Internal Medicine, Washington University, BJCIH Rm 11609, 425 S. Euclid Ave, Saint Louis, MO 63110, USA, scheller@wustl.edu, Phone: 314-747-7511. Dr. Ormond A MacDougald, Department of Molecular & Integrative Physiology, University of Michigan, 6313 Brehm Tower, 1000 Wall St, Ann Arbor, MI, 48105, USA, macdouga@umich.edu, Phone: 734-647-4880.

Specifically, we found that whereas caveolin 1 was necessary to mediate maximal stimulation of lipolysis in iWAT, overexpression of caveolin 1 was insufficient to rescue impaired BMAT signaling. Lastly, we tested the ability of BMAT to respond to 72-hour treatment with CL316,243 *in vivo*. This was sufficient to cause beiging of iWAT adipocytes and a decrease in iWAT adipocyte cell size. By contrast, adipocyte size in the tail BMAT and distal tibia remained unchanged. However, within the distal femur, we identified a subpopulation of BMAT adipocytes that underwent lipid droplet remodeling. This response was more pronounced in females than in males and resembled lipolysis-induced lipid partitioning rather than traditional beiging. In summary, BMAT has the capacity to respond to β-adrenergic stimuli, however, its responses are muted and BMAT generally resists lipid hydrolysis and remodeling relative to iWAT. This resistance is more pronounced in distal regions of the skeleton where the BMAT adipocytes are larger with little intervening hematopoiesis, suggesting that there may be a role for both cell-autonomous and microenvironmental determinants. Resistance to β-adrenergic stimuli further separates BMAT from known regulators of energy partitioning and contributes to our understanding of why BMAT is preserved in states of fasting and caloric restriction.

Graphical Abstract

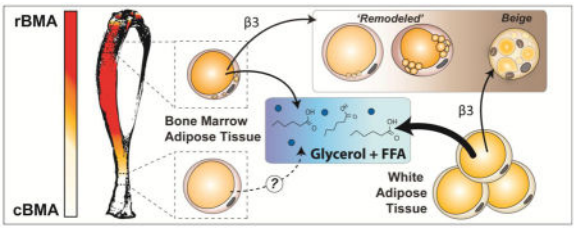

Keywords

marrow adipocytes; marrow adipose tissue; beiging; caloric restriction; fasting; lipolysis

1. INTRODUCTION

Recent work has established that, despite histologic similarities, bone marrow adipose tissue (BMAT) and white adipose tissue (WAT) are not the same. In addition, within BMAT there exists a population of ‘regulated’ and a population of ‘constitutive’ marrow adipocytes (1). Regulated bone marrow adipocytes (rBMAs) are currently defined as single cells interspersed within the red, hematopoietic bone marrow. By contrast, constitutive bone marrow adipocytes (cBMAs) form early in development, are larger in size, and appear histologically as confluent groups of cells with little intervening hematopoiesis. It remains unclear whether one simply represents a more immature version of the other, whether they are derived from distinct lineages, or whether their unique microenvironments dictate their function. Regulated BMAs tend to be enriched in the proximal and central parts of the skeleton. For example, BMAs exist in the region starting above the tibia/fibula junction (in rodents) and extending into the femur, pelvis, and lumbar vertebrae. Constitutive BMAs are enriched in the distal skeletal regions including the hands, feet, distal tibia, and tail vertebrae (if present).

One of the more intriguing differences between BMAT and WAT that has come to light in recent years is their differential response to nutrient deprivation and starvation (reviewed in (2,3)). Unlike WAT, BMAT accumulates in areas such as the femur and proximal tibia with chronic 30% calorie restriction in mice and anorexia in humans (4,5). This increase in BMAT is especially prominent when nutrient deprivation occurs during periods of skeletal growth, such as childhood or adolescence (4–6). During moderate starvation, after 10 to 14 days in rabbits for example, BMAT adipocytes also fail to mobilize their lipid reserve (7,8). It is only in the most severe circumstances, termed stage III of starvation (2), that a reduction of BMAT adipocyte size or serous degeneration of the bone marrow is observed (2,9).

While the underlying mechanism mediating the resistance of BMAs to dissolution is unclear, we know that breakdown of stored triacylglycerols within the adipocyte requires stimulation of lipolysis, generally mediated by catecholamine-based activation of β-adrenergic receptors (reviewed in (10,11)). Previous work has shown that regulated, but not constitutive, BMAs are depleted in mice after 21-day cold exposure – a model of elevated sympathetic tone and catecholamine release (1). However, the reason for this differential response is unclear. We hypothesized that cell-autonomous differences contribute to the divergent regulation of marrow adipocytes by β-adrenergic stimulation. The work presented in this paper is a synthesis of several experiments in rodents pertaining to the adrenergic regulation of BMAT and provides key insights into the site-specific properties and regulation of bone marrow adipocytes.

2. MATERIALS AND METHODS

2.1 Animal Use

All animal procedures were approved by the animal use and care committee at the University of Michigan. Animals were housed at 22°C on a 12-hour light/dark cycle with daily care by the Unit for Laboratory Animal Medicine.

2.1.1. 48-hour fast—Male Sprague-Dawley rats at 16- to 17-weeks of age or females at 18- to 20-weeks were placed in cages with aspen bedding with plastic chew toys and given free access to water, but not food, for 48-hours prior to euthanasia (isofluorane sedation followed by decapitation) and tissue collection.).

2.1.2. Cav1^{KO} Mice—Cav1$^{tm1Mls/J}$ mice (Jackson Labs, Bar Harbor, ME, USA; Stock no. 4585) were bred to B6129SJ2/J (Jackson Labs; Stock no. 101045) to generate heterozygotes (Razani, Combs et al. 2002). F1 heterozygote pairs were bred to generate cohorts of caveolin 1 knock-out (Cav1^{KO}) and wild-type animals for experimental analysis.

2.1.3. Cav1^{Tg} Mice—Caveolin-1 transgenic (Cav1^{Tg+}) mice were obtained from Dr. Ferruccio Galbiati at the University of Pittsburgh with the kind permission of Dr. Michael Lisanti (12). Male heterozygous transgenic mice were bred to C57BL6/J females (Jackson Labs; Stock no. 662). Tg+ and Tg− littermates were used to generate cohorts for analysis.

2.1.4. 72-hour CL316,243 Injection—Mice were injected with 5 μg/mouse CL316,243 (Sigma, Saint Louis, MO, USA) or saline control every 24-hours (time 0, 24, 48 hours) with euthanasia and tissue collection after 72-hours total.

2.2 Histology and adipocyte size quantification

Tissues were fixed in 10% neutral-buffered formalin for 24- to 48-hours (bones) or 4- to 5-days (adipose tissue). Bones were decalcified in 14% EDTA, pH 7.4 prior to staining and/or embedding. For the female rats and all mice, adipose and skeletal tissues were embedded in paraffin, sectioned, and stained with hematoxylin and eosin for adipocyte size quantification using the Metamorph® software package as described previously (13). For the 48-hour fast, adipocyte sizes of male rats were quantified using osmium staining and nano-computed-tomography as described previously (1,14).). For mouse adipocytes and rat BMAT, shifts in cell size distribution were determined within a standardized range of 200 to 3000 μm^2 (cell diameter of 16 to 62 μm). For rat iWAT the range was expanded up to 10,000 μm^2 (male) and 14,000 μm^2 (female). These ranges captured >95% of all adipocytes. Absolute adipocyte number was not quantified, but is unlikely to be different given the limited duration of the experiments (48- to 72-hours).

2.3. Western Blot

2.3.1. Acute signaling Studies (Rats)—Male Sprague-Dawley rats at 13- to 15-weeks of age were fasted overnight prior to intra-peritoneal injection of saline, 10 mg/kg isoproterenol hydrochloride (Tocris Bioscience/Bio-Techne, Minneapolis, MN, USA), 1 mg/kg CL316,243 (Sigma, Saint Louis, MO, USA), or 0.75 U/kg insulin (Humalin R, Eli Lilly). Rats were sedated with isofluorane after 14 minutes and decapitated after 15 minutes total. Inguinal WAT and BMAT were collected for analysis. For distal tibia BMAT, the tibiae were isolated and sectioned horizontally at the level of the tibia/fibula junction with a rotary tool as described previously (1). The marrow was removed from the distal tibial segments by centrifuging at 3000 x g for 1 minute at 4°C. The marrow plugs from the distal tibia were bisected horizontally and the most distal, ‘white’ portions pooled (two per animal) and used for protein extraction. This process took < 5 minutes per rat. BMAT and iWAT were then lysed simultaneously (see 2.3.3).

2.3.2. Acute signaling Studies (Mice)—Mice were fasted for four hours prior to intra-peritoneal injection with 0.3 mg/kg CL316,243 (Sigma, Saint Louis, MO, USA), 10 mg/kg isoproterenol hydrochloride (Tocris Bioscience/Bio-Techne, Minneapolis, MN, USA) or saline control. Mice were sedated with isofluorane after 14 minutes and euthanized after 15 minutes total. Inguinal WAT, femur, and tail vertebrae were collected for analysis. Whole femurs were isolated and cleaned mechanically with gauze. C3 to C6 tail vertebrae were individually separated and mechanically cleaned of overlying soft tissue using a sharpened tool to clean the crevices of the vertebral bone to remove any subcutaneous adipose tissue. By recruiting at least three people to work simultaneously, tissue collection was completed within ~5-minutes. All tissues from each mouse were then simultaneously processed for analysis (see 2.3.3).

2.3.3. General blotting protocol—SDS-PAGE and immunoblotting of tissue lysates was performed as described previously with minor modification (15). Specifically, rodent tissues were processed immediately after isolation using the Bullet Blender Gold® (Next Advance Inc, Averill Park, NY, USA) in 1.5 mL Safe-Lock tubes containing stainless steel beads in lysis buffer (1% SDS, 12.7 mM EDTA, 60 mM Tris-HCl; pH 6.8). Homogenized tissue lysates were heated to 95°C for 5 minutes prior to centrifugation at 20,000 x g for 20 minutes at 4°C. The cleared lysate above the pellet/beads and below the lipid layer was transferred to a new tube and stored at −80°C until needed. The BCA protein assay (Thermo Scientific, Waltham, MA, USA) was used to estimate the protein content of the lysate. Loading was adjusted so the control proteins were comparable between lanes. Antibodies and dilutions are listed in Supplementary Table 1. HRP-conjugated secondary antibody (GE HealthCare, Waukesha, WI, USA) was visualized with Western Lightning Plus (Perkin Elmer, Waltham, Massachusetts) or SuperSignal™ West Femto Maximum Sensitivity Substrate (Pierce, Rockford, IL, USA) titrated 1:1 – 1:3 with 1M Tris-HCl pH 8.0 to achieve optimal signal. Where noted, band density was quantified in FIJI using the gel analyzer plugin (16).

2.4 Adipocyte Isolation and Glycerol Assay

Adipocytes were isolated from iWAT, femur/tibia BMAT, and tail BMAT as described previously with the addition of 0.25% sodium citrate to the collagenase digestion solution to reduce loss of cells due to clotting (1). Isolated adipocytes were allowed to passively float to the surface of the isolation solution in 50 mL conical tubes for 5 minutes at 37°C, 5% CO_2. A glass pipet was used to remove ~90% of the infranatant and 10 mL of fresh Krebs-Ringer HEPES buffer containing 3% fatty-acid free BSA (KRBH) was added with gentle agitation. After a 5-minute incubation, this wash step was repeated twice to remove residual collagenase. After removal of the final wash the cells were resuspended in a minimal volume of KRBH so that the adipocytes remained densely packed. With gentle agitation, 100 μL of the cell suspension was aliquoted to 1.5 mL microtubes containing 400 μL of KRBH supplemented with the agonists of interest (total volume 500 μL). The cell suspensions were immediately incubated under constant rotation at 37°C for 60 minutes and then placed on ice for 10 minutes to stop the reaction. The tubes were centrifuged at 400 x g for 3 minutes to float the adipocytes and the infranatant was removed to a new tube. Free glycerol in the media was measured using a free glycerol determination kit (Cat. No. FG0100; Sigma, Saint Louis, MO, USA) and quantified relative to a standard curve from a glycerol standard solution.

2.5 RNA preparation

Rat tissues were isolated as described in 2.3.1 and placed in ice-cold Stat60 reagent in 1.5 mL safe-lock tubes (Eppendorf) containing 100 μL of a 0.9–2.0 mm blend of stainless steel beads (Next Advance, Averill Park, NY). Tissues were lysed by disrupting in a pre-cooled Bullet Blender Gold for 5 minutes at speed 8. Rat adipocytes were purified as described in 2.4 and re-suspended in Stat60. For all fatty tissues and cells, the Stat60 suspension was centrifuged at 3000 x g for 2 minutes to float the lipid and pellet debris. After centrifugation, the Stat60 solution below the lipid and above the pellet was moved to a new 1.5 mL tube and

used for RNA extraction. The RNA was pelleted as recommended by the manufacturer with the addition of a second ethanol wash step prior to re-suspension of the RNA pellet in water.

2.6 Quantitative PCR (qPCR)

For qPCR, 500 ng of total RNA was reverse-transcribed with RevertAid RT Kit reagents (Thermo Scientific, St Peters, MO, USA). Quantitative PCR was performed using qPCRBIO SyGreen 2X mix, Lo-Rox (PCR Biosystems, London, UK), on an Applied Biosystems QuantStudio 3 qPCR machine. Gene expression was calculated based on a cDNA standard curve within each plate and normalized to the expression of the geometric mean of the housekeeping genes *Ppia* and *Tbp* (17). Primer sequences were designed using the NCBI Primer-BLAST software (18) and are presented in Supplementary Table 2.

2.7 Osmium and micro computed-tomography

Mouse bones were fixed and decalcified as described in 2.2 prior to staining with osmium tetroxide for analysis of BMAT by micro computed-tomography, as described previously (1,19).

2.8 Immunohistochemistry

Tissues were fixed and embedded in paraffin prior to sectioning at 5 μm thickness. Sections were rehydrated in a series of xylenes and ethanol prior to antigen retrieval with sodium citrate buffer (10 mM Sodium citrate, 0.05% Tween 20, pH 6.0) for 20 minutes at 95°C. Slides were permeabilized for 10 min in 0.2% Triton-X 100 in PBS and blocked for 1-hour with 10% donkey serum. Primary antibody was made up in 2.5% donkey serum in TNT buffer (0.1 M Tris-HCl pH 7.4, 0.15 M sodium chloride, 0.05% Tween-20) and incubated overnight at 4°C. Secondary antibody was made in TNT buffer and incubated for 1-hour at room temperature. All washes between steps were performed in TNT buffer. Antibodies are detailed in Supplementary Table 1. For immunofluorescence, nuclei were counterstained with 1 μg/mL DAPI (Sigma, Saint Louis, MO, USA).

2.9 Statistics

Statistical analysis was done using GraphPad Prism 6 software (GraphPad Software, La Jolla, CA). Statistical tests are detailed in the figure legends. A p-value of <0.05 was considered statistically significant.

3. RESULTS

3.1 Acute fasting decreases cell size of BMAT adipocytes within the proximal tibia but not within the tail vertebrae

To test if BMAT responds to acute nutrient deprivation, in part mediated by adrenergic stimuli, male Sprague-Dawley rats at 16- to 17-weeks of age were fasted for 48-hours. Fasting decreased body mass by 9.1%, from 536±24 to 489±36 grams ($P = 0.004$) and glucose from 127±11 to 97±5 mg/dL ($P < 0.001$). Adipocytes within the iWAT from fasted animals demonstrated a significant increase in the proportion of small adipocytes and decrease in large adipocytes, reflecting an overall decrease in adipocyte size (Figure 1A,B).

The average iWAT cell volume decreased by 33%, from 126,000±42,000 μm^3 to 84,000±35,000 μm^3 when rounded to the nearest 1,000 μm^3. Within the skeleton, bone marrow adipocytes in the proximal tibia demonstrated a similar response, decreasing on average by 18%, from 16,000±2,000 μm^3 to 13,000±3,000 μm^3 (Figure 1C,D). By contrast, bone marrow adipocytes in the tail vertebrae did not undergo a decrease in size (Figure 1E,F).

Female Sprague-Dawley rats at 18- to 20-weeks of age were fasted for 48-hours with comparable results. Fasting decreased body mass by 8.4%, from 330±20 grams to 279±20 grams ($P = 0.001$) and glucose from 127±6 mg/dL to 89±8 mg/dL ($P < 0.001$). Inguinal WAT adipocytes from fasted animals demonstrated a trend toward decreased adipocyte size, with a significant increase in adipocytes with cross-sectional areas between 2500 and 4000 μm^2 relative to *ad lib* fed controls (Supplementary Figure 1A,B). The average iWAT cell volume decreased by 28%, from 260,000±51,000 μm^3 to 186,000±33,000 μm^3. The size of tibial BMAT adipocytes, at the level of the tibia/fibula junction, was significantly decreased in the fasted animals relative to the controls, with the average volume decreasing by 34%, from 19,000±5,000 μm^3 to 13,000±1,000 μm^3 (Supplementary Figure 1C,D). In tail vertebrae BMAT, fasting increased the proportion of adipocytes from 500 to 1000 μm^2 – registering as a non-significant 12% decrease in volume (Supplementary Figure 1E). However, overall, within the tail there were not significant changes in the proportion of small and large adipocytes relative to control females (Supplementary Figure 1F).

3.2 BMAT from distal tibia and tail vertebrae resists β-adrenergic stimulation of protein phosphorylation and lipolysis

Based on the resistance of tail cBMAs to fasting, we tested the ability of whole distal tibia BMAT, another region enriched with cBMAs, to respond to stimulation with β-adrenergic agonists and insulin *in vivo*. Male Sprague Dawley rats at 13- to 15-weeks of age were injected with insulin, isoproterenol, CL316,243, or saline control for 15 minutes prior to tissue isolation and analysis. The pan-β-adrenergic agonist isoproterenol stimulated phosphorylation of hormone sensitive lipase (HSL) in whole BMAT from the distal half of the region below the tibia/fibula junction (Fig. 2A). Relative to isoproterenol, phosphorylation of HSL in response to the selective β3-adrenergic agonist CL316,243 was reduced by approximately 90%. (Fig. 2A). Phosphorylation of perilipin (PLIN) was not observed in BMAT with either agonist at this time point (Fig. 2A). By contrast, both isoproterenol and CL316,243 stimulated robust phosphorylation of HSL and PLIN in inguinal WAT (Fig. 2A). Expression of adipose triglyceride lipase (ATGL) was present in both BMAT and iWAT (Fig. 2A). By contrast, expression of both CAV1 and CAV2, which contribute to coupling of β3-adrenergic receptors to adenylyl cyclase (20), was lower in BMAT than in iWAT (Fig. 2A).

Next, we purified primary adipocytes from the tail vertebrae (BMA tail), proximal tibia and femur (BMA T/F), and inguinal WAT (iWAT ads) of 16-week-old male Sprague Dawley rats to test adrenergic stimulation of lipolysis *ex vivo*. Isolated cells were treated in microtubes with constant rotation for 60 minutes with vehicle, CL316,243 or forskolin control. Purified BMAT adipocytes from the tail vertebrae failed to undergo lipolysis, as evidenced by

glycerol release, after β3-adrenergic stimulation with CL316,243 (Fig. 2B). Forskolin, the positive control, caused a significant 1.7-fold increase in glycerol release by tail BMAT adipocytes (Fig. 2B). By contrast, BMAT adipocytes purified from the proximal tibia and femur demonstrated a significant 1.5- and 1.3-fold response to both CL316,243 and forskolin respectively. Relative to BMAT, however, inguinal WAT adipocytes displayed an enhanced lipolytic response with a 17.2- and 15.4-fold increase in glycerol release after treatment with CL316,243 or forskolin (Fig. 2B).

3.3 Gene expression of β-adrenergic receptors in BMAT vs iWAT

We next examined gene expression of β-adrenergic receptors from purified BMAT adipocytes isolated from tail vertebrae (BMA Tail) and inguinal WAT (iWAT ads) of male Sprague Dawley rats at 16- to 17-weeks of age. The pattern of receptor expression in purified adipocytes was quite similar in both BMAT adipocytes and iWAT adipocytes (overall trend β3 > β1/β2) (Fig. 2C). In iWAT, *Adrb3* was expressed at significantly higher levels than *Adrb1* or *Adrb2*. This was not significant in BMAT. In summary, all three β-adrenergic receptor transcripts were detected in both BMAT adipocytes and iWAT adipocytes and, though *Adrb3* trended lower in BMAT relative to iWAT, this was not statistically significant.

3.4 Loss of caveolin-1 causes reduced phosphorylation of HSL and perilipin after β-adrenergic stimulation of iWAT

Existence of *Adrb3* in caudal vertebral cBMAs indicates that the non-responsivity to CL316,243 might due to functional deficiency. Thus, we hypothesized that defective coupling could explain impaired BMAT lipolysis in response to adrenergic stimuli. To determine whether caveolin 1 is required for β3-adrenergic stimulated lipolysis, we treated 24-week-old male Cav1 knock-out ($Cav1^{KO}$) mice and wild type littermate controls with saline or CL316,243 for 15 minutes prior to tissue isolation and analysis. Consistent with previous reports (21), we observed that β3-adrenergic stimulated protein phosphorylation of HSL and PLIN was significantly decreased in CAV1-null adipose tissue (Fig. 3A). Although stimulated phosphorylation of HSL was not observed in whole tail vertebrae, a small induction of P-HSL was observed in response to CL316,243 in the whole femur (Fig. 3B,C). This response was absent in whole femurs from the $Cav1^{KO}$ mice. We suspect that this response is due to lingering pieces of adipocyte-containing soft tissue at the proximal and distal ends of the whole femur, but cannot rule out a stimulated phosphorylation response in the regulated bone marrow adipocytes within.

3.5 β3-adrenergic stimulation causes lipolysis and beiging in inguinal WAT but not tail BMAT, regardless of CAV1 overexpression

We next tested whether transgenic overexpression of caveolin 1 was sufficient to rescue acute and chronic responses of BMAT to β3-adrenergic stimulation. $Cav1^{Tg+}$ mice had a significant 32% increase in CAV1 expression in tail vertebrae and 58% increase in whole femur relative to $Cav1^{Tg-}$ controls (Supplementary Figure 2A,B). Transgenic overexpression of *Cav1* did not cause an overt skeletal or BMAT phenotype in adult male or female mice at 16-weeks of age. Specifically, no significant differences were noted in tibial cortical morphology, cancellous bone volume, or BMAT volume in the proximal epiphysis, mid

tibia, or distal tibia (N = 5–9 per group, data not shown). Thus, to test whether overexpression of Cav1 was sufficient to promote the response of BMAT to β3-adrenergic stimulation, female $Cav1^{Tg-}$ and $Cav1^{Tg+}$ littermates at 9- to 10-weeks of age were treated with acute (15 minute) or chronic (72-hour) CL316,243. Control animals were injected with a matched volume of saline. Transgenic overexpression of Cav1 did not rescue the ability of acute CL316,243 to stimulate phosphorylation of HSL or PLIN in tail vertebrae (Supplementary Figure 2C). However, consistent with our results in rats (Fig. 2A), acute isoproterenol control was sufficient to stimulate phosphorylation of HSL in whole tail vertebrae from control mice (Supplementary Figure 2C). Phosphorylation of PLIN was also observed. In whole femurs, CL316,243-induced HSL phosphorylation did not differ between $Cav1^{Tg-}$ and $Cav1^{Tg+}$ mice, suggesting CAV1 expression in $Cav1^{Tg-}$ mice is not limiting for this response (Supplementary Figure 2D).

After 72-hour CL316,243 treatment, histologic assessment of cellular morphology revealed robust accumulation of multilocular, beige/BRITE adipocytes in the iWAT (Fig. 4A) as previously reported (22,23). By contrast, BMAT adipocytes in the tail vertebrae remained unilocular (Fig. 4A). The tibial marrow fat content was quantified using osmium tetroxide staining and micro computed-tomography as described previously (1,19). In the $Cav1^{Tg-}$ control animals the mean values of MAT volume were not significantly different with CL316,243 treatment in the proximal epiphysis, mid tibia (between the growth plate and tibia/fibula junction), or in the distal tibia (Fig. 4B–D). In $Cav1^{Tg+}$, CL316,243 significantly decreased BMAT in the proximal epiphysis and the mid tibia relative to saline-treated $Cav1^{Tg-}$ controls and $Cav1^{Tg+}$ animals, respectively (Fig. 4B,C). In $Cav1^{Tg-}$ control animals, CL316,243 caused a trend toward reduced BMAT in the mid tibia, but this was not significant. No change was noted in the distal tibia regardless of genotype or treatment (Fig. 4D). When quantified histologically, treatment of $Cav1^{Tg-}$ mice with CL316,243 caused iWAT adipocytes to decrease in size while cBMAs in the tail vertebrae remained unchanged (Fig. 4E,F). The same finding was observed in the $Cav1^{Tg+}$ mice (Fig. 4G,H). In summary, though it may have slightly enhanced the response of regulated BMAT adipocytes in the proximal tibia, transgenic overexpression of Cav1 did not rescue the ability of chronic CL316,243 to stimulate a decrease in cell size or remodeling of constitutive BMAT adipocytes in the tail.

3.6 β3-adrenergic stimulation causes lipid droplet remodeling of a subset of BMAT adipocytes

To validate these results in a 2nd mouse strain and more closely examine BMA changes using immunohistochemistry, male and female C3H/HeJ mice at 12-weeks of age were treated with CL316,243 for 72-hours to induce remodeling/beiging of peripheral adipose tissues. We then used microCT and immunohistochemistry to look for changes in BMAT adipocytes within the femur, tibia, and tail. Consistent with the results in C57BL6/J mice ($Cav1^{Tg-}$ and $Cav1^{Tg+}$), treatment with CL316,243 was sufficient to induce beiging and a decrease in adipocyte cell size in iWAT (Fig. 5D, Supplementary Fig. 3A,B). Average iWAT adipocyte cell volume decreased by 41% in both male (P = 0.118) and female mice (P = 0.006). By contrast, based on osmium staining and microCT, CL316,243 did not induce a significant decrease in tibial BMAT in the mid tibia (growth plate to tibia/fibula junction) or

distal tibia in either male or female mice (Fig. 5A,B). However, adipocyte size analysis in the proximal tibia revealed a minor, but statistically significant, increase in cells of 200 to 400 μm^2 in size, suggesting a small decrease in BMAT cell size (−10 to 11% change in average volume) (Supplementary Fig. 3).

To examine this more closely, we performed perilipin staining and immunohistochemical analysis in the iWAT, femur, and tail vertebrae. This revealed the presence of 'remodeled' BMAT adipocytes in the distal femur (Fig. 5C,D). Remodeling was defined as having three or more smaller lipid droplets associated with a large droplet (see for example Fig. 5D,E). At baseline in the femur, 5.6+/−3.9% of the BMAT adipocytes in males and 8.9+/−4.4% in females had a remodeled appearance. After treatment with CL316,243 for 72-hours the proportion of multilocular/remodeled cells increased to 27.5+/−10.0% in the females, while the males remained at 6.8+/−4.3%. The smaller lipid droplets around the "multilocular" BMAT adipocytes were generally associated with a larger lipid droplet instead of being uniformly distributed, as occurred in beige adipocytes within the iWAT (Fig. 6E). These types of remodeled cells were not prevalent in the confluent BMAT near the middle of the C3 to C5 tail vertebrae, however, at high resolution, a few cells could be found to have very small budding droplets (Fig. 6E).

4. DISCUSSION

4.1 Resistance to conventional lipolytic stimuli

After a 48-hour fast, which engages the endogenous lipolytic machinery, we observed a 28 to 33% decrease in iWAT adipocyte cell volume. Tibial BMAT adipocyte volume decreased by 18% (males) or 34% (females). The response in the tail BMAT was limited or absent. Similarly, stimulation with CL316,243 for 72-hours, a β3-selective agonist, caused a 27 to 41% decrease in iWAT cell volume in control mice. Tibial BMAT underwent a non-significant 9 to 11% decrease. No change was noted in tail vertebrae. Responses to acute treatment with isoproterenol or CL316,243 were also suppressed or absent in BMAT depending on skeletal site. Together, this promotes a paradigm by which BMAT adipocytes are capable of responding to β-adrenergic signals, but their response is relatively muted when compared to peripheral white adipocytes. This diminished response is more pronounced in areas of cBMAs such as the tail vertebrae relative to rBMAs in the proximal tibia and femur (Fig. 6).

These results contribute to our understanding of why BMAT is preserved during caloric restriction and acute starvation, relative to peripheral white adipose tissues (4,5,7,8,24). Functionally, the response of BMAT may mimic the adipose tissue around the lymph nodes (reviewed in (25)). Perinodal adipocytes respond less readily to lipolytic signals such as norepinephrine and are instead stimulated to undergo lipolysis by cytokines that are released by local immune cells (26,27). This means that perinodal adipocytes are able to fuel the local immune response without depending on circulating energy reserves (28), enabling immune responses even in times of peripheral energy deficit (29). Like perinodal fat, BMAT adipocytes have a muted, site-specific response to conventional adrenergic lipolytic stimuli (Fig. 6). This may prompt preservation of lipid in times of acute starvation and disassociate BMAT from peripheral energy demand in favor of contributions to local processes. At some

point, however, chronic, near terminal starvation causes BMA dissolution (2). This likely provides a final energy reserve to promote survival.

4.2 Mechanisms of signal attenuation

When stimulated directly, the response of BMAT appears to benefit from engagement of β1- or β2-adrenergic receptors, perhaps in addition to β3, to induce downstream phosphorylation of lipolytic proteins including HSL and PLIN. This is consistent with previous work showing that isoproterenol stimulates fatty acid release by bone marrow *in vivo* (30). By contrast, β3-adrenergic stimulation alone, which is conventionally regarded as the major regulator of lipolysis in peripheral white adipose tissue, was relatively ineffective in BMAT from the femur and tibia and responses were mostly absent in BMAT of the tail vertebrae. We hypothesized that this could be explained by differences in adrenergic receptor expression or coupling through caveolin 1. Though there was a trend toward reduced *Adrb3* in purified BMAT adipocytes from the tail vertebrae relative to iWAT adipocytes (~60% less), we found that the overall expression pattern and proportion of *Adrb1*, *Adrb2*, and *Adrb3* was relatively similar between BMAT and iWAT adipocytes in 16- to 17-week old male Sprague Dawley rats. Though this difference in *Adrb3* was not significant in our study, microarray data of BMAT adipocytes purified from mouse femur and tibia revealed a comparable ~60% decrease of *Adrb3* expression in BMAT relative to epididymal WAT adipocytes at 6-, 14-, and 18-months of age in male C57BL/6J mice (4.8±0.3 *vs* 10.9±0.4, $P < 0.001$, GEO dataset GSE25905 from (31)). Future studies are needed to extend these findings and to clarify adrenergic receptor expression and function on BMAT adipocytes from proximal and distal skeletal regions.

In addition to expression of adrenergic receptors, we examined coupling of Adrb3 through caveolae by knock-out and overexpression of caveolin 1 *in vivo*. In these experiments we found that whereas caveolin 1 was necessary for maximal WAT lipolysis, transgenic overexpression was insufficient to rescue defects in BMAT lipolysis. Future work is clearly needed to define the signals that promote energy release by BMAT adipocytes and enhance resistance to β-adrenergic cues. It also remains unclear whether adrenergic signals prompt unique responses in BMAs, for example, alternate coupling through small G-proteins to regulate something other than lipolysis. Reduced capacity for simulated lipolysis could also be due to enhanced basal rates, due perhaps to local functional demands or increases in futile cycling.

4.3 Cell size of BMAT relative to WAT

As has been previously reported (1,9), the cell size of the BMAT adipocyte is remarkably constrained. Within the present studies across adult mice and rats, in both males and females, at all skeletal sites, and regardless of chemical treatment, the average BMAT adipocyte diameter ranged from only 23.8 to 40.2 μm. By contrast, in the same animals, iWAT adipocyte diameter ranged from 27.7 to 78.9 μm. The relationship between adipocyte sizes in BMAT and iWAT size was variable. Specifically, BMAT adipocytes were smaller than iWAT adipocytes in rats, consistent with previous findings in rabbits (9); however, both were comparable in size in the mouse. Regulated BMAs in the proximal tibia were generally smaller than constitutive BMAs in the distal tibia and tail (tail > distal tibia > proximal

tibia). This is slightly different than previous work in rabbits where distal and proximal BMAT adipocytes in femur, humerus, and tibia were relatively comparable in size (9). However, it may be notable that in mice this pattern was slightly different in female mice (tail = distal tibia > proximal tibia) relative to males (tail > distal tibia = proximal tibia). The significance of this observation and its applicability across species remains unclear at this point, but may reflect differences in rBMA and cBMA distribution between males and females.

4.4 Does BMAT respond to β3-adrenergic stimulation by beiging?

While we observed lipid droplet remodeling in some BMAT adipocytes in response to CL316,243, we do not have evidence at this time to suggest that this is due to true beiging. Morphologically, BMA remodeling was quite different from traditional beiging observed in the iWAT adipocytes (small lipid globules uniformly filling the cytoplasm) and instead consisted primarily of the larger central lipid droplet becoming encircled by several smaller lipid droplets. Although we observed UCP1 staining of brown and beige adipose tissues, we were unable to observe a consistent signal in antibody-based UCP1 staining of remodeled BMAs above that present in bone from UCP1 knock-out mice (data not shown). This may due to limitations of our technique within bone marrow or cross-reaction of the antibody with other UCP proteins (*ex.* UCP2). In the future, lineage tracing approaches in which UCP1 drives expression of a reporter gene are needed to clarify this point.

It remains unknown why females responded more readily than males to CL316,243. It is notable, however, that at baseline in both sexes, ~5–9% of the femoral BMAT adipocytes within a 2D cross-section had cytoplasmic regions of small lipid droplets. Since this was analyzed in 5 μm-thick paraffin sections, but the average diameter of bone marrow adipocyte is ~30 μm, the fraction of cells with small droplets at baseline is likely much higher regardless of sex (ie. 30–50% or more). This is consistent with three-dimensional electron microscopic reconstructions of BMAT adipocytes which show small cytoplasmic lipid droplets around a central lipid globule, which are polarized toward sinusoidal blood vessels, into areas of hematopoiesis, and near the bone interface (32). In total, our results suggest that a subset of BMAT adipocytes has the capacity for remodeling of their lipid droplet in response to 72-hour β3-adrenergic stimulation. Our current evidence supports a model in which these small droplets regulate energy partitioning to surrounding cells, as they do not uniformly mimic the phenotype of traditional ‘beige’ iWAT cells. Future work is needed to determine if longer, sustained adrenergic signals (> 72-hours) or additional cues are capable of inducing beiging and/or remodeling of BMAT.

4.5 Relevance of our work to the rBMA and cBMA hypothesis

This work supports the notion that cells within the proximal, hematopoietic-rich skeletal regions (“rBMAs”) are more susceptible to remodeling and lipolysis (1). Cell autonomous features such as increased lipid droplet partitioning in rBMAs may contribute to this enhanced response. We also observed the expected increase in cell size of tail cBMAs relative to proximal tibia rBMAs.

5. CONCLUSIONS

Given the relative resistance of BMAT to traditional β-adrenergic stimuli, additional work is needed to identify the unique inter- and intracellular mechanisms that mediate hydrolysis of BMAT energy stores. Beyond this, it remains unclear what this energy is used for. Logic would dictate that local energy partitioning may be important for processes including hematopoiesis and bone formation/turnover. However, at some point during the most severe stages of starvation, we know that BMAT can be leveraged as a final energy reserve to promote survival (2). The identification of signals present (or lacking) during these BMAT functional contexts will provide new tools for pharmacologic regulation of BMAT and contribute to our understanding of both skeletal and systemic energy metabolism.

Supplementary Material

Refer to Web version on PubMed Central for supplementary material.

Acknowledgments

This work was supported by grants from the National Institutes of Health including R24-DK092759 (O.A.M.), K99-DE024178 (E.L.S.), and R00-DE024178 (E.L.S.). W.P.C. was supported by a Lilly Innovation Fellowship Award, and a Postdoctoral Research Fellowship from the Royal Commission for the Exhibition of 1851 (United Kingdom), and currently is supported by a Career Development Award (MR/M021394/1) from the Medical Research Council (United Kingdom). We would like to thank Dr. Karl Jepsen and Basma Khoury for their help with nano-computed tomography.

ABBREVIATIONS

BMAT	bone marrow adipose tissue
WAT	white adipose tissue
rBMA	regulated bone marrow adipocyte
cBMA	constitutive bone marrow adipocyte
HSL	hormone sensitive lipase
PLIN	perilipin
ATGL	adipose triglyceride lipase
KRBH	Krebs-ringer HEPES buffer

BIBLIOGRAPHY

1. Scheller EL, Doucette CR, Learman BS, Cawthorn WP, Khandaker S, Schell B, et al. Region-specific variation in the properties of skeletal adipocytes reveals regulated and constitutive marrow adipose tissues. Nat Commun. 2015 Aug 6.6:7808. [PubMed: 26245716]
2. Devlin MJ. Why does starvation make bones fat? Am J Hum Biol. 2011 Oct; 23(5):577–585. [PubMed: 21793093]
3. Ghali O, Al Rassy N, Hardouin P, Chauveau C. Increased bone marrow adiposity in a context of energy deficit: the tip of the iceberg? Front Endocrinol (Lausanne). 2016 Sep 16.7:125. [PubMed: 27695438]

4. Devlin MJ, Cloutier AM, Thomas NA, Panus DA, Lotinun S, Pinz I, et al. Caloric restriction leads to high marrow adiposity and low bone mass in growing mice. J Bone Miner Res. 2010 Sep; 25(9): 2078–2088. [PubMed: 20229598]
5. Cawthorn WP, Scheller EL, Learman BS, Parlee SD, Simon BR, Mori H, et al. Bone marrow adipose tissue is an endocrine organ that contributes to increased circulating adiponectin during caloric restriction. Cell Metab. 2014 Aug 5; 20(2):368–375. [PubMed: 24998914]
6. Hamrick MW, Ding KH, Ponnala S, Ferrari SL, Isales CM. Caloric restriction decreases cortical bone mass but spares trabecular bone in the mouse skeleton: implications for the regulation of bone mass by body weight. J Bone Miner Res. 2008 Jun; 23(6):870–878. [PubMed: 18435579]
7. Tavassoli M. Differential response of bone marrow and extramedullary adipose cells to starvation. Experientia. 1974 Apr 15; 30(4):424–425. [PubMed: 4858192]
8. Bathija A, Davis S, Trubowitz S. Bone marrow adipose tissue: response to acute starvation. Am J Hematol. 1979; 6(3):191–198. [PubMed: 484542]
9. Cawthorn WP, Scheller EL, Parlee SD, Pham HA, Learman BS, Redshaw CM, et al. Expansion of bone marrow adipose tissue during caloric restriction is associated with increased circulating glucocorticoids and not with hypoleptinemia. Endocrinology. 2016 Feb; 157(2):508–521. [PubMed: 26696121]
10. Collins S. β-Adrenoceptor Signaling Networks in Adipocytes for Recruiting Stored Fat and Energy Expenditure. Front Endocrinol (Lausanne). 2011; 2:102. [PubMed: 22654837]
11. Duncan RE, Ahmadian M, Jaworski K, Sarkadi-Nagy E, Sul HS. Regulation of lipolysis in adipocytes. Annu Rev Nutr. 2007; 27:79–101. [PubMed: 17313320]
12. Bryant KG, Camacho J, Jasmin JF, Wang C, Addya S, Casimiro MC, et al. Caveolin-1 overexpression enhances androgen-dependent growth and proliferation in the mouse prostate. Int J Biochem Cell Biol. 2011 Sep; 43(9):1318–1329. [PubMed: 21601007]
13. Parlee SD, Lentz SI, Mori H, MacDougald OA. Quantifying size and number of adipocytes in adipose tissue. Meth Enzymol. 2014; 537:93–122. [PubMed: 24480343]
14. Khoury BM, Bigelow EM, Smith LM, Schlecht SH, Scheller EL, Andarawis-Puri N, et al. The use of nano-computed tomography to enhance musculoskeletal research. Connect Tissue Res. 2015 Apr; 56(2):106–119. [PubMed: 25646568]
15. Cawthorn WP, Bree AJ, Yao Y, Du B, Hemati N, Martinez-Santibañez G, et al. Wnt6, Wnt10a and Wnt10b inhibit adipogenesis and stimulate osteoblastogenesis through a β-catenin-dependent mechanism. Bone. 2012 Feb; 50(2):477–489. [PubMed: 21872687]
16. Schindelin J, Arganda-Carreras I, Frise E, Kaynig V, Longair M, Pietzsch T, et al. Fiji: an open-source platform for biological-image analysis. Nat Methods. 2012 Jun 28; 9(7):676–682. [PubMed: 22743772]
17. Vandesompele J, De Preter K, Pattyn F, Poppe B, Van Roy N, De Paepe A, et al. Accurate normalization of real-time quantitative RT-PCR data by geometric averaging of multiple internal control genes. Genome Biol. 2002 Jun 18.3(7):RESEARCH0034. [PubMed: 12184808]
18. Ye J, Coulouris G, Zaretskaya I, Cutcutache I, Rozen S, Madden TL. Primer-BLAST: a tool to design target-specific primers for polymerase chain reaction. BMC Bioinformatics. 2012 Jun 18.13:134. [PubMed: 22708584]
19. Scheller EL, Troiano N, Vanhoutan JN, Bouxsein MA, Fretz JA, Xi Y, et al. Use of osmium tetroxide staining with microcomputerized tomography to visualize and quantify bone marrow adipose tissue in vivo. Meth Enzymol. 2014; 537:123–139. [PubMed: 24480344]
20. Sato M, Hutchinson DS, Halls ML, Furness SG, Bengtsson T, Evans BA, et al. Interaction with caveolin-1 modulates G protein coupling of mouse β3-adrenoceptor. J Biol Chem. 2012 Jun 8; 287(24):20674–20688. [PubMed: 22535965]
21. Martin S, Fernandez-Rojo MA, Stanley AC, Bastiani M, Okano S, Nixon SJ, et al. Caveolin-1 deficiency leads to increased susceptibility to cell death and fibrosis in white adipose tissue: characterization of a lipodystrophic model. PLoS ONE. 2012 Sep 26.7(9):e46242. [PubMed: 23049990]
22. Lee YH, Petkova AP, Mottillo EP, Granneman JG. In vivo identification of bipotential adipocyte progenitors recruited by β3-adrenoceptor activation and high-fat feeding. Cell Metab. 2012 Apr 4; 15(4):480–491. [PubMed: 22482730]

23. Contreras GA, Lee YH, Mottillo EP, Granneman JG. Inducible brown adipocytes in subcutaneous inguinal white fat: the role of continuous sympathetic stimulation. Am J Physiol Endocrinol Metab. 2014 Nov 1; 307(9):E793–9. [PubMed: 25184993]
24. Bredella MA, Fazeli PK, Miller KK, Misra M, Torriani M, Thomas BJ, et al. Increased bone marrow fat in anorexia nervosa. J Clin Endocrinol Metab. 2009 Jun; 94(6):2129–2136. [PubMed: 19318450]
25. Craft CS, Scheller EL. Evolution of the Marrow Adipose Tissue Microenvironment. Calcif Tissue Int. 2016 Jul 1; 100(5):1–15. [PubMed: 27671989]
26. Mattacks CA, Pond CM. Interactions of noradrenalin and tumour necrosis factor alpha, interleukin 4 and interleukin 6 in the control of lipolysis from adipocytes around lymph nodes. Cytokine. 1999 May; 11(5):334–346. [PubMed: 10328873]
27. MacQueen HA, Pond CM. Immunofluorescent localisation of tumour necrosis factor-alpha receptors on the popliteal lymph node and the surrounding adipose tissue following a simulated immune challenge. J Anat. 1998 Feb; 192(Pt 2):223–231. [PubMed: 9643423]
28. Pond CM, Mattacks CA. The source of fatty acids incorporated into proliferating lymphoid cells in immune-stimulated lymph nodes. Br J Nutr. 2003 Mar; 89(3):375–383. [PubMed: 12628033]
29. Pond CM. Interactions of Adipose and Lymphoid Tissues. In: Fantuzzi G, Mazzone T, editorsAdipose Tissue and Adipokines in Health and Disease. Totowa, NJ: Humana Press; 2007. 133–150.
30. Tran MA, Lac DT, Berlan M, Lafontan M. Interplay of alpha-2 and beta adrenoceptors in the control of free fatty acid release from bone marrow adipose tissue. J Pharmacol Exp Ther. 1984 Jul; 230(1):228–231. [PubMed: 6086878]
31. Liu LF, Shen WJ, Ueno M, Patel S, Kraemer FB. Characterization of age-related gene expression profiling in bone marrow and epididymal adipocytes. BMC Genomics. 2011 May 5.12:212. [PubMed: 21545734]
32. Robles H, Park S, Joens M, Fitzpatrick J, Craft CS, Scheller EL. Characterization of the bone marrow adipocyte niche with three-dimensional electron microscopy. Bone. 2018 Jan 21.

HIGHLIGHTS

- When compared to white adipose tissue, bone marrow adipose tissue has diminished lipolytic responses to acute β-adrenergic stimuli
- Resistance to β-adrenergic signals is more pronounced in distal skeletal regions where BMAT adipocytes are larger with little intervening hematopoiesis
- Transgenic overexpression of caveolin 1 is insufficient to rescue the response of bone marrow adipocytes to β-adrenergic stimuli in mice
- β3-adrenergic agonist CL316,243 stimulates lipid droplet remodeling in a subset of bone marrow adipocytes located in the femur of females

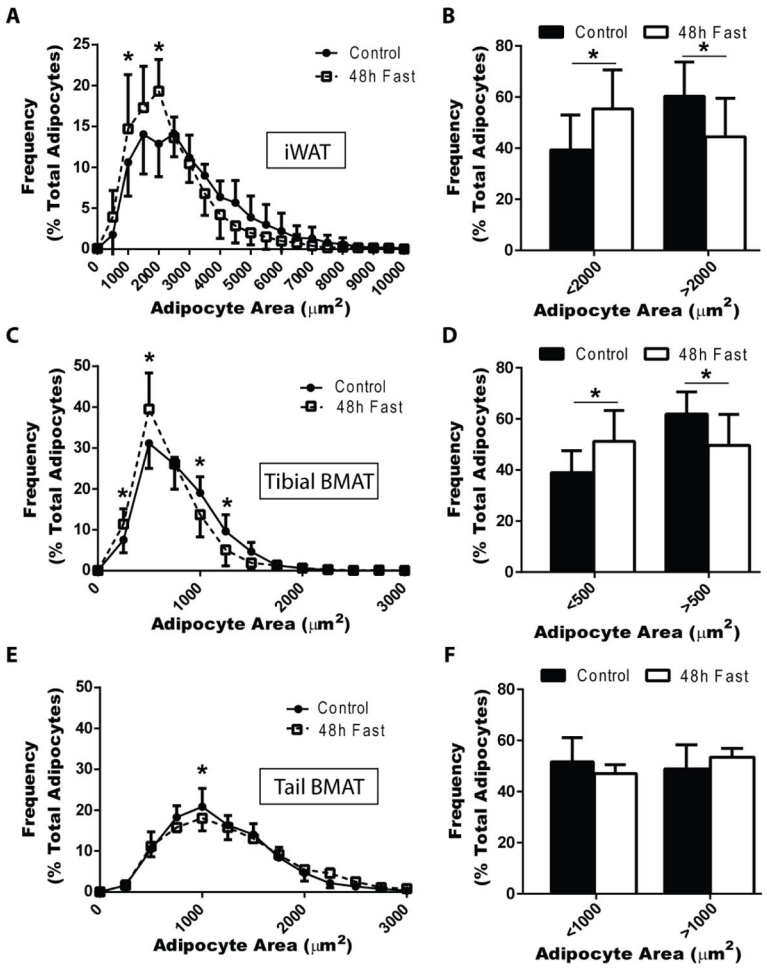

Figure 1. A 48-hour fast decreases tibial, but not tail, bone marrow adipocyte size in male rats

Male Sprague-Dawley rats of 16- to 17-weeks in age were fasted for 48-hours (N = 12 fed, 6 fasted). Adipocyte sizes were quantified using nanoCT in tissues from fed and fasted animals. The results were then expressed as the proportion of adipocytes in the listed size ranges (see histograms A, C, E) and bar graphs (B, D, F). Absolute adipocyte number was not quantified, but is unlikely to be different given the limited duration of the experiments. **(A,B)** Inguinal white adipose tissue (iWAT) adipocytes decreased in size after a 48-hour fast as shown by a left shift in the histogram (A) and an increase in the proportion of small adipocytes (B). **(C,D)** Bone marrow adipose tissue adipocyte at the proximal tibia (Tibial BMAT) also decreased in size. **(E,F)** Bone marrow adipose tissue in the tail vertebrae (Tail BMAT) remained relatively unchanged. Presented as mean ± standard deviation. Statistical tests include (A,C,E) 2-way ANOVA with Sidak's multiple comparisons test and (B,D,F) two-tailed t-test. *P<0.05

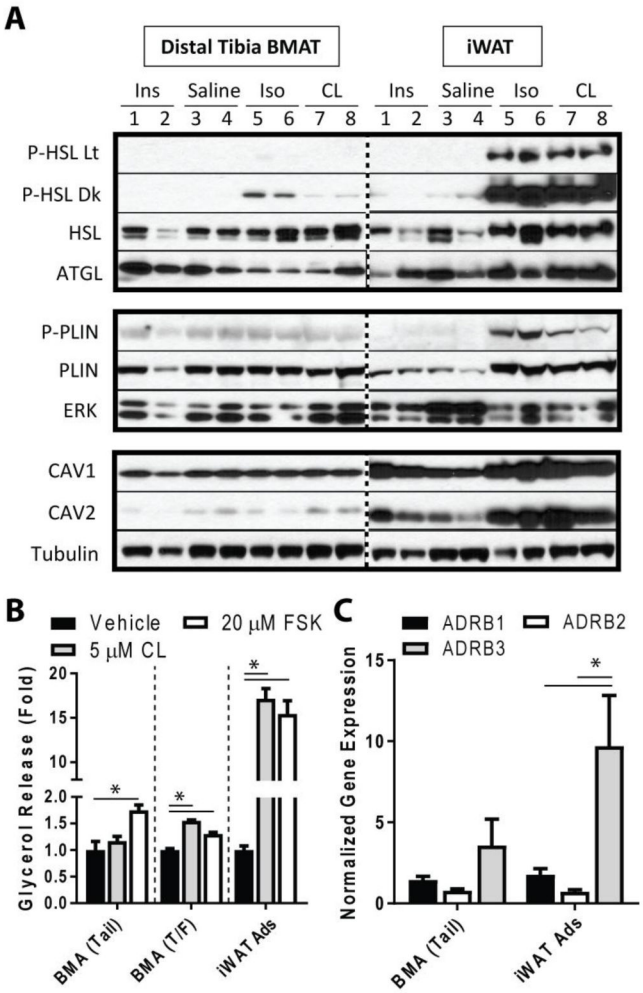

Figure 2. Adrenergic-stimulated lipolysis in bone marrow adipose tissue

Male Sprague-Dawley rats at 13 to 15 weeks of age were fasted overnight prior to intra-peritoneal injection of saline (N = 4), 0.75 U/kg insulin (N = 4), 10 mg/kg isoproterenol (N = 4), or 1 mg/kg CL316,243 (N = 3). Tissues were harvested after 15 minutes. **(A)** Representative western blots show two rats per each treatment. Horizontal lanes have been cropped from the same gel/exposure and can be compared across the dotted line. Column numbers correspond to rat numbers 1 through 8. Lt = light burn, Dr = darker image of the same blot. HSL = hormone sensitive lipase. ATGL = adipose triglyceride lipase. PLIN = perilipin. CAV = caveolin. **(B)** Primary adipocytes were isolated from the tail vertebrae (BMA Tail), proximal tibia and femur (BMA T/F) and inguinal white adipose tissue (iWAT Ads) of 16-week-old male Sprague-Dawley rats. Cells were treated with the indicated compounds for 1-hour and then the media was analyzed for glycerol release, representative of stimulated triglyceride breakdown/lipolysis. CL = CL316,243. FSK = forskolin. Adipocytes pooled from 12 animals, technical replicate N = 3 (BMA Tail and BMA T/F) and N = 6 (iWAT). Expressed as fold stimulation relative to vehicle. Mean+/−SEM. One-way ANOVA with Tukey's multiple comparisons test to compare vs vehicle control. *$p<0.05$ as indicated. **(C)** Gene expression of the β-adrenergic receptors from purified

BMAT adipocytes from the tail vertebrae (BMA Tail) and iWAT from 16- to 17-week old male Sprague-Dawley rats that were *ad lib* fed (N = 6 BMA, 8 iWAT). Receptor expression normalized to the geometric mean of reference genes *Tbp* and *Ppia*. Mean±SEM. Statistics: two-way ANOVA with Sidak's multiple comparisons test. *p<0.05, a=significant vs same receptor in BMAT.

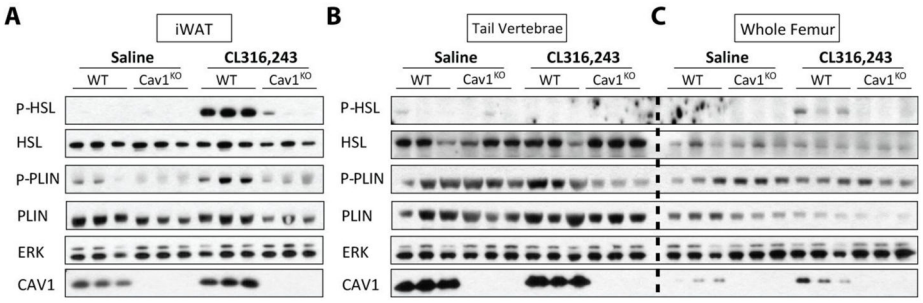

Figure 3. β3-adrenergic stimulated lipolysis in whole tissues from Caveolin 1 knock-out mice

Western blot of protein expression in 24-week-old male wild-type (WT) and CAV1 knock-out ($Cav1^{KO}$) mice treated with saline or 0.3 mg/kg CL316,243 for 15 minutes. **(A)** Inguinal white adipose tissue (iWAT), **(B)** whole tail vertebrae mechanically cleaned of residual soft tissue (tail vertebrae), and **(C)** mechanically cleaned whole femur (whole femur). Three representative animals shown per group (N = 6 WT saline, 5 WT CL316,243, 4 $Cav1^{KO}$ saline, 5 $Cav1^{KO}$ CL316,243).

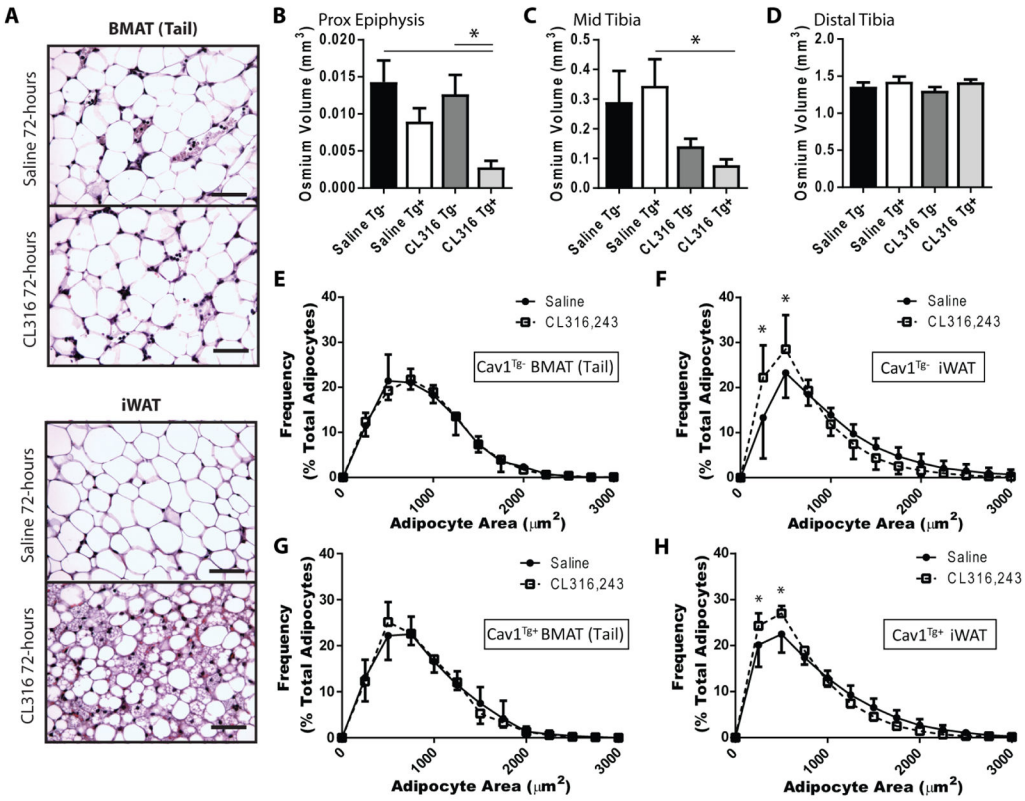

Figure 4. β3-adrenergic stimulation causes lipolysis and beiging in inguinal WAT but not tail BMAT, regardless of CAV1 overexpression

Female caveolin-1 transgenic ($Cav1^{Tg+}$) mice and $Cav1^{Tg-}$ littermate controls at 10-weeks of age were injected with CL316,243 every 24-hours for 72-hours. These mice are on a C57BL/6J background. **(A)** Representative histology of marrow adipocytes within the tail vertebrae (BMAT Tail) and inguinal white adipose tissue (iWAT) from control animals. Hematoxylin and eosin stain. 40X Magnification. Scale bar = 50 μm. Quantification of tibial marrow fat volume using osmium tetroxide in the **(B)** proximal epiphysis, **(C)** between the growth plate and tibia/fibula junction, and **(D)** in the distal tibia. Mean±SEM. Non-parametric Kruskal-Wallis test with Dunn's multiple comparisons. *P<0.05. (**EH)** Adipocyte cell size distribution of inguinal white adipose tissue (iWAT) and bone marrow adipose tissue (BMAT) from tail vertebrae of female control or $Cav1^{Tg}$ mice. 2-way ANOVA with Sidak's multiple comparisons test. Presented as mean±standard deviation. *P<0.05. N = 9 saline WT, 6 saline Tg, 8 CL316 WT, 6 CL316 Tg.

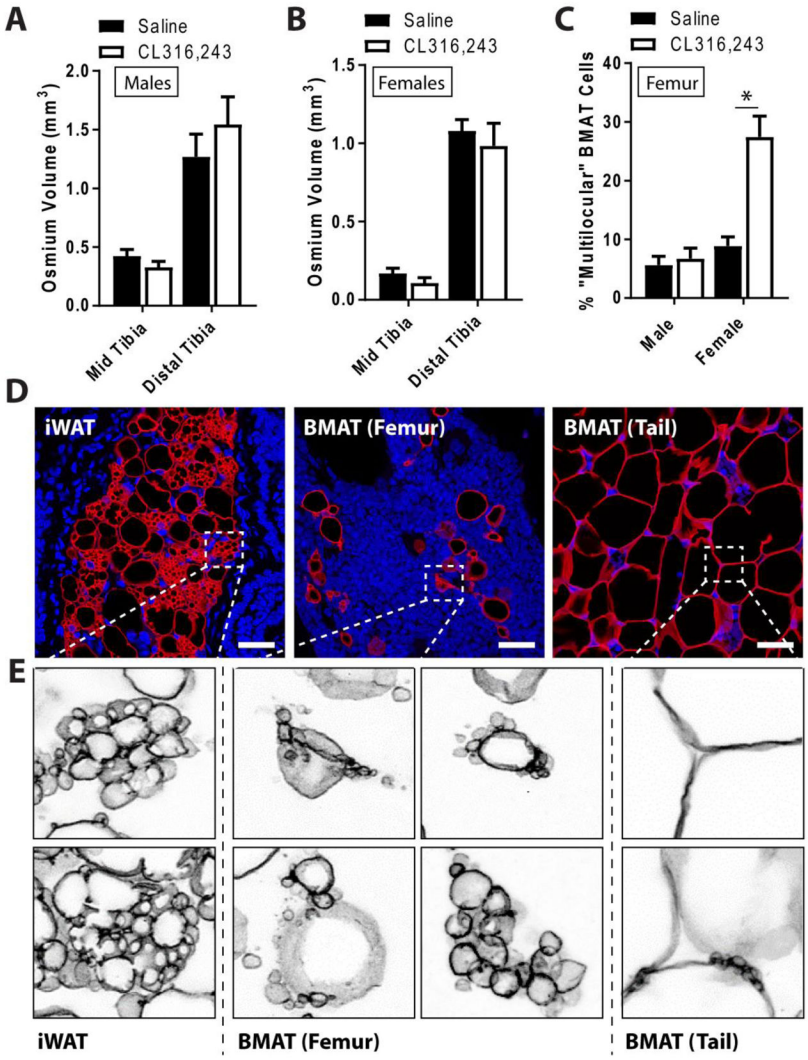

Figure 5. β3-adrenergic induced changes occur more readily in areas of hematopoietic-rich BMAT within the proximal tibia and femur

Male and female C3H/HeJ mice at 12-weeks of age were treated with saline or CL316,243 once per day for 72-hours (N = 7–8 per group). **(A,B)** Quantification of tibial marrow fat volume using osmium tetroxide in mid tibia (between the growth plate and tibia/fibula junction) and in the distal tibia. Mean±SEM. Two tailed t-test within each skeletal site. **(C)** Quantification of 'remodeled' BMAT adipocytes in the distal femur. Remodeling was defined as having three or more smaller lipid droplets associated with a large droplet (aka "multilocular"). Two tailed t-test within male or female. **(D)** Representative immunohistochemical stain for perilipin (red) and dapi (blue) in mice treated with CL316,243. Scale bar = 30 μm. **(E)** Representative beige iWAT adipocytes, remodeled BMAT adipocytes from the femur, and tail BMAT adipocytes. Perilipin stain inverted, presented in black.

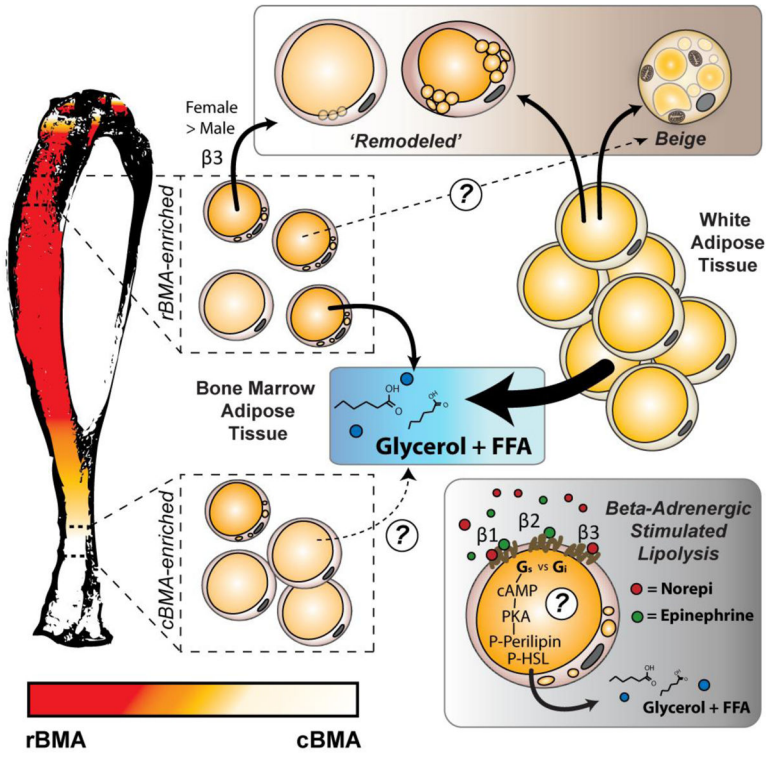

Figure 6. Summary

Relative to distal sites such as the distal tibia and tail, in proximal skeletal regions BMAT adipocytes tend to be smaller with an increased incidence of smaller lipid droplets within their cytoplasm. This may increase their surface area and facilitate hydrolysis of triglyceride in response to β-adrenergic stimuli contributing to their designations as regulated or constitutive bone marrow adipocytes (rBMA, cBMA – reviewed in (REF)). These cells are also capable of responding to sustained β3-adrenergic stimulation by increasing the number of small lipid droplets in their cytoplasm, particularly in females ('remodeling'). In general, remodeled BMAT adipocytes do not resemble conventional beige adipocytes. Relative to white adipose tissue, the response of BMAT to direct beta-adrenergic stimuli is significantly reduced regardless of site. In general, BMAT responds more readily to pan-β-adrenergic agonist isoproterenol than to β3-specific agonist CL316,243 suggesting that BMAT may be more sensitive physiologically to the 'fight or flight' catecholamine epinephrine than to the canonical neural-derived catecholamine norepinephrine.